Mon. Not. R. Astron. Soc. **350,** 609–614 (2004) doi:10.1111/j.1365-2966.2004.07670.x

On the use of X-rays to determine dynamical properties of elliptical galaxies

Luca Ciotti⋆ and Silvia Pellegrini
Astronomy Department, University of Bologna, via Ranzani 1, 40127 Bologna, Italy

Accepted 2004 January 26. Received 2004 January 23; in original form 2003 December 23

ABSTRACT

The extended and X-ray-emitting interstellar medium of early-type galaxies is often used as a tool to determine their total mass M and stellar orbital anisotropy β profiles, based on the hypothesis of hydrostatic equilibrium for the hot gas. Here we investigate the effects that deviations from equilibrium have on M and β estimates, by using simple analytical calculations and hydrodynamical simulations representative of gas-rich galaxies. We show that the deviations of the X-ray-determined $\beta^{\rm est}$ and $M^{\rm est}$ from the true values are linked by a remarkably simple relation; in particular, M is underestimated if β is overestimated. Also, more radially anisotropic orbital distributions than the true one are deduced in presence of gas infall velocities of the order of the local stellar velocity dispersion (as are likely in the central regions of galactic cooling flows). The results of this analysis are applied to the most thoroughly investigated bright elliptical, NGC 4472. First we show that $\beta^{\rm est}$ recently derived from X-rays corresponds to a galaxy that is unstable by radial orbit instability. Then, assuming as true β and M the optically derived values, we show that the differences $\beta^{\rm est}-\beta$ and $M^{\rm est}-M$ agree with the predictions found here in the case of lack of hydrostatic equilibrium, which points to the latter as a possible explanation for the discrepancies. This analysis casts doubts on the possibility of using X-ray information to determine accurately the dynamical properties of bright X-ray-emitting ellipticals, at least within their $R_{\rm e}$.

Key words: cooling flows – galaxies: elliptical and lenticular, cD – galaxies: kinematics and dynamics – galaxies: structure – X-rays: galaxies – X-rays: ISM.

1 INTRODUCTION

Since its discovery in the late 1970s (Fabbiano 1989), the presence of an extended and X-ray-emitting interstellar medium (ISM) in early-type galaxies raised the hope of having a new powerful and reliable tool to determine the dynamical properties of these galaxies, in particular their mass profile and total mass out to large radii ($\sim$10 optical effective radii $R_{\rm e}$). In the simplest and commonly adopted approach, these determinations assume a spherical mass distribution. Then, the most general expression for the momentum equation of the gas is

$$\frac{k}{\mu m_{\rm p}}\frac{1}{\rho}\frac{{\rm d}\rho T}{{\rm d}r}+\mathcal{V}=-g, \qquad (1)$$

where T and ρ are the radial profiles of the ISM temperature and density, $m_{\rm p}$ is the proton mass, μ is the mean molecular weight and $g=GM(r)/r^2$ is the total gravitational field. $\mathcal{V}$ includes all the non-hydrostatic terms and, for simplicity, we do not consider other pressure terms such as the magnetic one (see, however, Section 4).

⋆E-mail: luca.ciotti@unibo.it

Thus, in hydrostatic equilibrium, $T(r)$ and $\rho(r)$ – which in principle can be inferred from the X-ray surface brightness profile through deprojection, using also spectral information (e.g. Forman, Jones & Tucker 1985; Trinchieri, Fabbiano & Canizares 1986) – are linked to the total mass profile by the well-known formula (Fabricant, Lecar & Gorenstein 1980)

$$M(r)=-r\frac{kT}{G\mu m_{\rm p}}\left(\frac{{\rm d}\log\rho}{{\rm d}\log r}+\frac{{\rm d}\log T}{{\rm d}\log r}\right). \qquad (2)$$

Forman et al. (1985) made the first total mass determinations using this approach, for a sample of early-type galaxies with *Einstein* data extending out to radii of $\sim$50 kpc. They obtained large mass values implying that dark matter should be present in large quantities ($M/L_B\sim 25$–$100\,{\rm M}_\odot/{\rm L}_{B,\odot}$). However, uncertainties in the ρ and T profiles were so large that mass values could be even as low as those derived from optical measurements (Trinchieri et al. 1986; Fabbiano 1989), which typically give $M/L_B\sim 12\,{\rm M}_\odot/{\rm L}_{B,\odot}$ within $R_{\rm e}$ (Saglia, Bertin & Stiavelli 1992).

Mass profiles can in fact also be derived from the observed stellar velocity dispersion profiles $\sigma_{\rm p}(R)$; these extend out to $\sim$(1–2)$R_{\rm e}$ in a few best cases (e.g. Kronawitter et al. 2000). In this context, a common approach is to use the Jeans equations: for a spherical

model described by a phase-space distribution function $f = f(E, L^2)$, the relevant equation is

$$\frac{1}{\rho_*}\frac{\mathrm{d}\rho_*\sigma_\mathrm{r}^2}{\mathrm{d}r} + \frac{2\beta\sigma_\mathrm{r}^2}{r} = -g \tag{3}$$

(e.g. Binney & Tremaine 1987). Here ρ_* is the stellar density profile and $\beta(r) = 1 - \sigma_\mathrm{t}^2(r)/2\sigma_\mathrm{r}^2(r)$, where σ_r is the radial stellar velocity dispersion and $\sigma_\mathrm{t}^2 = \sigma_\varphi^2 + \sigma_\vartheta^2$ is the total tangential stellar velocity dispersion. $\beta(r)$ describes the radial trend of anisotropy in the stellar velocity dispersion tensor, which is radially anisotropic where $0 < \beta < 1$, tangentially anisotropic where $\beta < 0$ and isotropic where $\beta = 0$. For assumed visible and dark density profiles and a specified radial trend of $\beta(r)$, equation (3) is solved to derive $\sigma_\mathrm{r}^2(r)$; then by projection one obtains $\sigma_\mathrm{p}(R)$ to be compared with the observed one. As is well known, in the absence of a physically motivated choice for $\beta(r)$, this method suffers from a 'dark matter–β degeneracy': a sufficient amount of orbital anisotropy can mimic the presence of a massive dark matter halo (e.g. Tonry 1983). Observationally, $\beta(r)$ can be derived from the deviation of the line profiles from a Gaussian (e.g. Gerhard et al. 1998), but this process requires high-quality data and care in analysis. In fact, the use of the hot ISM to derive dynamical quantities was very welcomed also because it is exempt from this degeneracy problem.[1]

In hydrostatic equilibrium, the two conditions (1) (with $\mathcal{V} = 0$) and (3), holding for the gas and the stars lying in the same total gravitational field g, allow us to determine $M(r)$ and $\beta(r)$ uniquely, when coupled with the knowledge of the four observables $T(r)$, $\rho(r)$, $\rho_*(r)$ and $\sigma_\mathrm{p}(R)$. For example, by eliminating g from (1) and (3) one obtains a relation linking gas and stellar properties only (Fabricant, Kent & Kurtz 1989):

$$\frac{k}{\mu m_\mathrm{p}\rho}\frac{\mathrm{d}\rho T}{\mathrm{d}r} = \frac{1}{\rho_*}\frac{\mathrm{d}\rho_*\sigma_\mathrm{r}^2}{\mathrm{d}r} + \frac{2\beta\sigma_\mathrm{r}^2}{r}. \tag{4}$$

Then, one can use the equation above to derive $\beta(r)$ using information coming from X-ray observations, as attempted recently by Mathews & Brighenti (2003a, hereafter MB03).

The lack of reliable ISM density and temperature profiles has been a severe limitation to the use of X-rays as a probe of the galactic potential and of stellar dynamical quantities. This was first overcome partially thanks to *ROSAT* observations. Currently, quite accurate T and ρ profiles are being derived from *Chandra* and *XMM–Newton* observations (e.g. Sun et al. 2003). In addition, in a few cases *Chandra* data have already shown signs of departure from hydrostatic equilibrium in hot gas coronae (e.g. Jones et al. 2002). Therefore a timely question is how reliable the X-ray estimate of dynamical quantities can be.

In this paper we address the problem of the accuracy of the X-ray-based total mass $M(r)$ and $\beta(r)$ determination when the hydrostatic equilibrium hypothesis is assumed but it does not hold. Our analysis relies upon the use of the relevant hydrodynamical equations, while we do not discuss technical problems related to the extraction of physical quantities from the observations, such as the well-known ill-posed problem of Abel inversion for observed data (e.g. Tikhonov & Goncharsky 1987).

[1] Note that, in other approaches (e.g. Bertin et al. 1994), the anisotropy profile is not a function to be specified by independent arguments, but derives from the physical picture on which the model is based.

2 ESTIMATES OF MASS AND ORBITAL ANISOTROPY WHEN $\mathcal{V} \neq 0$

In the most general case ($\mathcal{V} \neq 0$) the physically correct analog of equation (4) is

$$\frac{k}{\mu m_\mathrm{p}\rho}\frac{\mathrm{d}\rho T}{\mathrm{d}r} + \mathcal{V} = \frac{1}{\rho_*}\frac{\mathrm{d}\rho_*\sigma_\mathrm{r}^2}{\mathrm{d}r} + \frac{2\beta\sigma_\mathrm{r}^2}{r}. \tag{5}$$

Instead, by erroneously assuming hydrostatic equilibrium, one uses an equation involving β^est:

$$\frac{k}{\mu m_\mathrm{p}\rho}\frac{\mathrm{d}\rho T}{\mathrm{d}r} = \frac{1}{\rho_*}\frac{\mathrm{d}\rho_*\sigma_\mathrm{r}^2}{\mathrm{d}r} + \frac{2\beta^\mathrm{est}\sigma_\mathrm{r}^2}{r}. \tag{6}$$

Therefore the difference between the estimated and the true anisotropy profiles is given by

$$\beta^\mathrm{est} - \beta = -\frac{r}{2\sigma_\mathrm{r}^2}\mathcal{V}. \tag{7}$$

Following the same reasoning, the equation that should be used to derive the total mass profile $M(r)$ is equation (1), while using it with $\mathcal{V} = 0$ one derives an estimated mass M^est given by

$$M^\mathrm{est} = M + \frac{r^2}{G}\mathcal{V}. \tag{8}$$

Note that, although M^est and β^est derive from two independent procedures, the deviation in the mass estimate is linked to that in the β estimate by a remarkably simple relation:

$$\frac{M^\mathrm{est}(r)}{M(r)} - 1 = -\frac{2r\sigma_\mathrm{r}^2(r)[\beta^\mathrm{est}(r) - \beta(r)]}{GM(r)}. \tag{9}$$

Thus, for example, $M^\mathrm{est} < M$ wherever $\beta^\mathrm{est} > \beta$.

In general, the modulating factor $2r\sigma_\mathrm{r}^2/GM$ in equation (9) depends on the exact slope of the stellar density profile, on the presence of dark matter and on $\beta(r)$ [via $\sigma_\mathrm{r}(r)$]. The radial behaviour of this factor for a few representative cases is given in Fig. 1. Within $\sim 0.2R_\mathrm{e}$ the factor is very sensitive to the shape of the density profile,

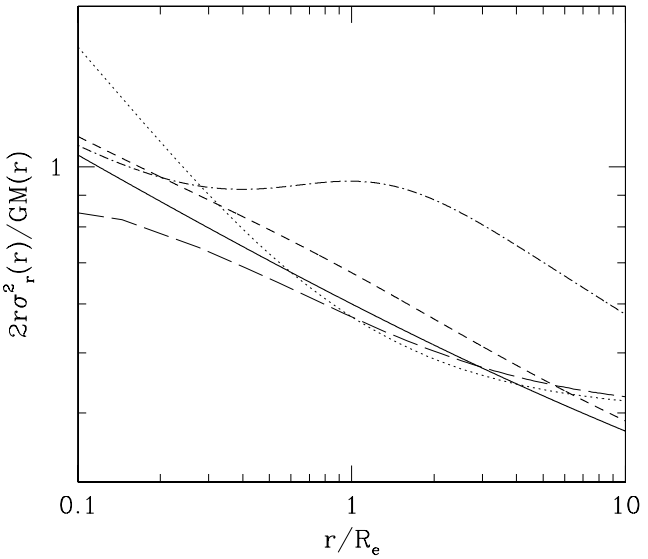

Figure 1. The modulating factor of equation (9) is plotted for the isotropic Hernquist (dotted line), Jaffe (long-dashed line) and de Vaucouleurs (solid line) density profiles. The dot–dashed line represents a maximally anisotropic de Vaucouleurs model (see Section 2). The short-dashed line is an isotropic stellar de Vaucouleurs model plus a Hernquist dark matter halo 5 times as massive as the stellar component; the mass enclosed within R_e is the same for the two components (see Section 2).

as shown by the cases of the de Vaucouleurs (1948), Jaffe (1983) and Hernquist (1990) isotropic models (respectively the solid, long-dashed and dotted lines). In addition, Fig. 1 also shows that this dependence is not trivially linked to the radial behaviour of the ρ_* profile, since $\rho_*(r) \propto r^{-3/4}$, r^{-2} and r^{-1} respectively for the de Vaucouleurs (Ciotti 1991), Jaffe and Hernquist models. The inner shape of the factor can be derived, however, from the asymptotic analysis discussed by Bertin, Ciotti & Del Principe (2002).

The short-dashed line in Fig. 1 refers to an isotropic stellar de Vaucouleurs model coupled to a dark matter halo that is described by a Hernquist profile and is 5 times as massive as the stellar component; the mass enclosed within R_e is the same for the two components (which implies a core radius for the Hernquist model of $2.47R_e$). Compared with the corresponding pure stellar model (solid line) there is a small increase in the modulating factor.

When $\beta > 0$ the factor is larger than in the isotropic case: for example, when β is radially constant,[2] as adopted in some modellings (see e.g. Section 3), and the density distribution is $\rho_* \propto r^{-\gamma}$, the factor is $1/(\gamma - 1 - 0.5\beta)$. In Fig. 1 the dot–dashed line refers to a de Vaucouleurs profile with $\beta(r)$ radially varying according to the Osipkov–Merritt parametrization (Osipkov 1979; Merritt 1985). In the central region, the effect of such a $\beta(r) = r^2/(r^2 + r^2{}_a)$ (where r_a is the anisotropy radius) is a small increase of the modulating factor with respect to the isotropic case (solid line). In the external regions an idea of the full range of the factor values is derived by comparing the cases of isotropic and anisotropic orbital distributions for a de Vaucouleurs profile (solid and dot–dashed lines respectively). In fact, for this profile, the choice of $r_a \simeq R_e$ adopted for Fig. 1 gives the maximum allowed level of anisotropy, based on stability arguments (Ciotti & Lanzoni 1997, see also Section 3).

In summary, outside the effective radius the modulating factor is everywhere <0.7; for the 'maximally' anisotropic case, it is everywhere <1. Within R_e it is again everywhere $\lesssim 1$, except for the Hernquist model. Therefore for most models 'errors' on M (i.e. $M^{\rm est}/M - 1$) are less than or approximately equal to the β deviations (i.e. $\beta^{\rm est} - \beta$).

In the next sections we estimate the difference $\beta^{\rm est} - \beta$ in equation (7), first qualitatively (Section 2.1) and then quantitatively by using numerical models of hot gas flows for X-ray-bright galaxies (Section 2.2).

2.1 Qualitative analysis

We assume that the hot ISM filling the galactic potential well has velocity, density and temperature u, ρ and T. Usually, in the case of galactic flows, a mass source rate $\alpha\rho_*(r)$ is present in the $\mathcal{V}$ term, due to the stellar mass losses (e.g. Ciotti et al. 1991). For an inviscid fluid, the $\mathcal{V}$ term is then written as

$$\mathcal{V} = \frac{\partial u}{\partial t} + \frac{1}{2}\frac{{\rm d}u^2}{{\rm d}r} + \frac{\alpha\rho_* u}{\rho}. \tag{10}$$

We consider first equation (7) in the simplest case, namely the stationary case with $\alpha = 0$; then

$$\beta^{\rm est} - \beta = -\frac{r}{4\sigma_r^2}\frac{{\rm d}u^2}{{\rm d}r}. \tag{11}$$

This shows that when the velocity decreases with increasing radius *in magnitude*, i.e. when ${\rm d}u^2/{\rm d}r < 0$, then $\beta^{\rm est}(r) > \beta(r)$. This is the case of the central regions in cooling flows. If, instead, the velocity increases in modulus with increasing radius, then $\beta(r)$ is underestimated. This could be the case of galactic winds. Note that fairly large differences $\beta^{\rm est} - \beta$ are expected when u^2 varies by $\sim\sigma_r^2$ over a characteristic length of the order of r.

When $\alpha > 0$, these results are reinforced in two cases: when the gas is inflowing ($u < 0$) with a velocity decreasing with radius (${\rm d}u^2/{\rm d}r < 0$), then even more radially anisotropic orbits are deduced; and when the gas is outflowing ($u > 0$) with a velocity increasing with radius (${\rm d}u^2/{\rm d}r > 0$), then even more tangentially anisotropic orbits are deduced. In the other cases the $\alpha\rho_*/\rho$ term may have a competing effect on the ${\rm d}u/{\rm d}r$ term that depends on the magnitude of the source function α.

All the results above can be converted straightforwardly into results concerning mass estimates by using equation (9).

The X-ray-brightest galaxies, for which better quality data are available and dynamical studies can be attempted, contain large quantities of hot gas and are supposed to host inflows for which ${\rm d}u^2/{\rm d}r < 0$. In their inner regions (well within $\sim R_e$) the gas can reach high velocities, up to the local sound speed, while $u \sim 0$ outside R_e (e.g. Ciotti et al. 1991). Therefore it is expected that more radially anisotropic orbits than the true one are deduced from X-ray observations of the central regions; $\beta^{\rm est}$ derived outside R_e should be reliable. More quantitative estimates follow below.

2.2 Quantitative results

Here we study the effect of the full $\mathcal{V}$ term given in equation (10). For this investigation, two gas dynamical models are used, resulting from the numerical simulations of time-evolving galactic gas flows by Pellegrini & Ciotti (1998) and representative of hot gas-rich galaxies. In principle, one should use a numerically computed right-hand side of equation (10). However, in order to reduce the numerical noise due to spatial and temporal derivatives over a finite grid, the $\mathcal{V}$ term is obtained from equation (1), so that

$$\beta^{\rm est} - \beta = \frac{r}{2\sigma_r^2}\left(g + \frac{k}{\mu m_p \rho}\frac{{\rm d}\rho T}{{\rm d}r}\right). \tag{12}$$

Similarly,

$$\frac{M^{\rm est}}{M} = -\frac{k}{g\mu m_p \rho}\frac{{\rm d}\rho T}{{\rm d}r}. \tag{13}$$

In fact, for the galaxy models we know g and β. As representative cases we consider (1) a bright inflowing galaxy ($L_B = 7 \times 10^{10} {\rm L}_\odot$, $R_e = 9.0$ kpc, central $\sigma = 287$ km s^{-1} and a dark halo 9 times as massive as the stellar component); and (2) a less massive galaxy in which the inflow is confined within $0.1R_e$ ($L_B = 2.2 \times 10^{10}$ L$_\odot$, $R_e = 4.4$ kpc, central $\sigma = 210$ km s^{-1} and a dark halo twice as massive as the stellar component). The underlying galaxy model is isotropic ($\beta = 0$).

The top panel of Fig. 2 shows the radial trend of the gas velocity at the end of the simulations (corresponding to an elapsed time of 15 Gyr). The second panel shows whether any term on the right-hand side of equation (10) gives a dominant contribution to $\mathcal{V}$. Since the gas flows have reached a quasi-steady state after 15 Gyr, the $\partial u/\partial t$ term is negligible, and only the radial trend of the advective/source term ratio is plotted. For the largely inflowing galaxy the advective term dominates in the central region and becomes comparable to the source term at $\sim R_e$, while for the partial wind model the two terms keep comparable. For both models the two terms produce a deviation in the same sense, since they are both negative in the inflowing region and positive in the outflowing region.

[2] Any consideration of the physical consistency of this assumption is left aside here: see, e.g. Camm (1952).

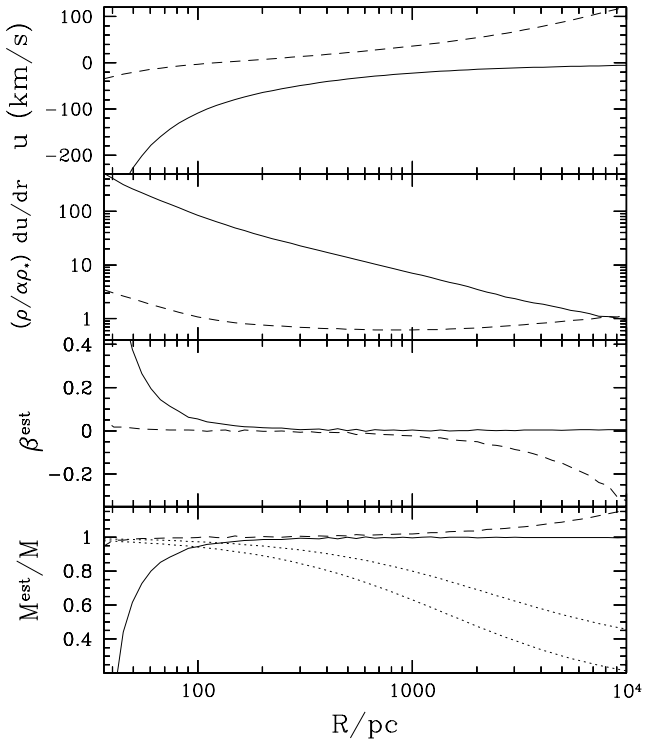

Figure 2. For a global inflow (in a galaxy with $L_B = 7.1 \times 10^{10}\,\mathrm{L}_\odot$, solid line) and a partial wind (in a galaxy with $L_B = 2.2 \times 10^{10}\,\mathrm{L}_\odot$, dashed line; more details on the model galaxies are given in Section 2.2), from top to bottom the panels show the radial trends of the gas flow velocity, the ratio between the advective and the source terms in equation (10), $\beta^{\rm est}$, and $M^{\rm est}$ normalized to the true total mass. In the lowest panel the dotted lines give the stellar mass profiles of the two model galaxies (again normalized to the total mass; see Section 2.2 for more details).

In the lowest two panels, Fig. 2 shows what $\beta^{\rm est}$ and $M^{\rm est}$ would be derived from X-ray observations. Overall, the trends of $\beta^{\rm est}$ agree with the qualitative analysis of Section 2.1 and, as expected, $\beta^{\rm est}$ is >0 for the central gas inflowing region. For the galaxy hosting a global inflow, decidedly more radially anisotropic orbits than the true one would be deduced by neglecting the gas velocity; correspondingly, $M^{\rm est} < M$ would be derived for the central galactic region [equation (9) and Fig. 2]. Outside the inflow region, $\beta^{\rm est}$ is small and $M^{\rm est} \sim M$, consistent with the predictions for low gas velocities.

3 THE CASE OF NGC 4472

The X-ray-bright Virgo galaxy NGC 4472 has been chosen since the early days of the field for detailed investigations of its dynamical properties using X-ray data (Thomas 1986; Trinchieri et al. 1986; Loewenstein 1992; Bertin, Pignatelli & Saglia 1993; Bertin & Toniazzo 1995; Irwin & Sarazin 1996). The study based on the most recent and extensive data set is that of MB03 (see also Mathews & Brighenti 2003b). MB03 employed equation (4) to relate $\beta(r)$ and $T(r)$. They used $\rho(r)$ derived from Abel-inverted *Chandra*, *ROSAT* and *Einstein* surface brightness profiles, $T(r)$ derived from deprojection of *ROSAT* and *Chandra* data, the observed $\sigma_{\rm p}(R)$ from Bender, Saglia & Gerhard (1994) and Fried & Illingworth (1994), and $\rho_*(r)$ resulting from fitting the observed brightness profile with a de Vaucouleurs law (but in the central regions the density profile was assumed to steepen as $r^{-0.9}$).

Adopting a radially constant $\beta^{\rm est}$ for the modelling, the value $\beta^{\rm est} = 0.71 \pm 0.15$ was derived, while the optically determined $\beta(r)$ within $R_{\rm e}$ is everywhere $\lesssim 0.34$ (Kronawitter et al. 2000). That is, $\beta^{\rm est}$ is about twice as large as the maximum β found from optical data. Conversely, assuming the optically determined $\beta(r)$ of Kronawitter et al. (2000), a $T(r)$ higher than the observed value is obtained. Commenting on this result, MB03 state that: 'This strong preference for radial stellar orbits must be understood in terms of the formation history of massive elliptical galaxies. Conversely, if the smaller, optically determined β is indeed correct, we are led to the important conclusion that the temperature profile $T(r)$ of the hot ISM in NGC 4472 must differ from that indicated by X-ray observations, or that the hot gas is not in hydrostatic equilibrium.'

Here we argue that, if problems with the several steps involved in the modelling of the data can be excluded, the last possibility of lack of hydrostatic equilibrium is strongly favoured. In fact a simple stability argument rules out as unphysical such a high X-ray-derived $\beta^{\rm est}$ value. In the case of a constant anisotropy parameter, the radial orbit instability indicator (Polyachenko & Shukhman 1981; Fridman & Polyachenko 1984) turns out to be

$$\frac{2K_{\rm r}}{K_\vartheta + K_\varphi} = \frac{1}{1-\beta^{\rm est}} \simeq 3.45, \qquad (14)$$

where $K_{\rm r}$ and $K_\vartheta + K_\varphi$ are respectively the total radial and tangential kinetic energies. A galaxy is unstable because of radial orbit instability when this indicator is $\gtrsim 1.7 \pm 0.25$; therefore the value calculated in equation (13) is well outside the stability regime. Note that, even when inserting the maximum value of $\beta(r) = 0.34$ derived by Kronawitter et al. (2000) in equation (13), the indicator is ≈ 1.5, safely in the stability regime. The criterion above has been proved to be obeyed essentially by all galaxy models to which it has been applied, even including massive dark haloes (e.g. Stiavelli & Sparke 1991; Nipoti, Londrillo & Ciotti 2002; Bertin & Trenti 2003; see also Saha 1991).

Additional considerations argue in favour of the hypothesis of lack of hydrostatic equilibrium to explain the inconsistencies between X-ray- and optically derived orbital anisotropy. In fact, there is also a deviation between the X-ray- and the optically derived mass for NGC 4472, and the two discrepancies (concerning β and M) are related as predicted by equation (9), as shown in the following. Having discarded the X-ray-derived $\beta^{\rm est}$ as unphysical, we assume that the optical estimate of β is the correct one. Then, equation (9) predicts the X-ray-derived $M^{\rm est}$ to underestimate the true mass M. More specifically, the expected value of $M^{\rm est}/M$ can be derived from the results for the de Vaucouleurs models in Fig. 1. For a range of values of the modulating factor within $R_{\rm e}$ of $\sim$0.5–1 and for $\beta^{\rm est} - \beta = 0.4$, then $M^{\rm est}/M = 0.8$–0.6 is given by equation (9). What $M^{\rm est}$ derives from the X-ray data? The best-fitting total mass profile $M^{\rm est}(r)$ determined from equation (2), with the same $T(r)$ and $\rho(r)$ as used by MB03, is a one-component de Vaucouleurs mass profile out to $r = R_{\rm e}$, with a total constant mass-to-light ratio of $M^{\rm est}/L_B = 7$ (Mathews & Brighenti 2003b). M/L_B estimates were also derived from optical studies based on high-quality photometric and kinematic data extending out to $\sim 0.5 R_{\rm e}$. The M/L_B determined from one-component constant mass-to-light ratio axisymmetric dynamical models is 9.2, for the central galactic region, when rescaled to the distance adopted by MB03 (van der Marel 1991). Another analysis used spherical self-consistent two-component models (Saglia et al. 1992). The models selected at a 3σ confidence level have $M/L_B = 10.1$–14.6 within $R_{\rm e}$, when rescaled to the MB03

distance.[3] These optically determined M values, if taken as true values, imply that $M^{\rm est}$ underestimates the true mass M. More precisely, $M^{\rm est}/M = 0.76$ and 0.69–0.48 when adopting respectively van der Marel's and Saglia et al.'s results, in remarkable agreement with the predictions above ($M^{\rm est}/M = 0.8$–0.6). Therefore the hypotheses of (i) correct optical estimates of β and M and (ii) departure from hydrostatic equilibrium of the hot ISM give a consistent explanation for the discrepancies of the X-ray-derived $\beta^{\rm est}$ and $M^{\rm est}$ values. In particular, these hypotheses account for the fact that $\beta^{\rm est}$ is an overestimate and $M^{\rm est}$ is an underestimate, and also for the *size* of the discrepancies with the true β and M.

4 DISCUSSION AND CONCLUSIONS

We have investigated the effect that deviations from hydrostatic equilibrium have on X-ray estimates of the total mass M and the orbital anisotropy parameter β via the 'standard' equations (2) and (4). We have found the following results.

(i) In the most general case, the deviations of $\beta^{\rm est}$ and $M^{\rm est}$ from the true values are linked by a remarkably simple relation. In particular, the mass is underestimated if β is overestimated. Also, for the most common density and orbital anisotropy distributions, with or without a massive dark halo, the $\beta^{\rm est}$ deviations are larger than the 'errors' on M at all radii $\gtrsim 0.2 R_{\rm e}$.

(ii) In the stationary case without mass/momentum sources/sinks, more radially anisotropic orbits than the true one are deduced for the central regions of gas-inflowing galaxies. Instead, $\beta(r)$ is underestimated for outflowing regions where the velocity increases with radius, as in galactic winds. When mass sources are present, the results above are reinforced in the inflow and in the wind cases. In the other cases the mass source term may have a competing effect.

(iii) The full time-dependent problem is investigated with the aid of numerical simulations reproducing gas-rich galaxies. The results are consistent with the simple qualitative predictions. $\beta^{\rm est}$ decidedly overestimates the true value (and $M^{\rm est}$ underestimates it) if derived from the central region where gas is inflowing with a large velocity, while outside it $\beta^{\rm est} \sim \beta$ and $M^{\rm est} \sim M$.

(iv) $\beta^{\rm est}$ and $M^{\rm est}$ derived for the most thoroughly investigated bright elliptical galaxy (NGC 4472), for which the best X-ray data are available, are considered as a representative application of our results. We show that the high $\beta^{\rm est}$ recently derived is unphysical. We also note a discrepancy in the X-ray- and optically-derived masses within $R_{\rm e}$. Assuming as true β and M the optically-derived values, the β overestimate implies (when applying our results to non-hydrostatic equilibrium) an M underestimate in remarkable agreement with $M^{\rm est} - M$. Of course, one cannot exclude that a different modelling of the X-ray and optical data would be able to produce a $\beta(r)$ profile consistent with the observed one, in the hydrostatic equilibrium hypothesis. However, this would reveal a degeneracy in the procedure and undermine the possibility of uniquely deriving dynamical information from the X-ray data.

(v) Note that equations (7)–(9) describe the deviations of $\beta^{\rm est}$ and $M^{\rm est}$ from the true values even when sources of pressure additional to the thermal one are effective (such as magnetic and radiation pressure). In fact, if these are accounted for explicitely in equations (2) and (4), then equations (7)–(9) remain unaltered. If these are not accounted for, again equation (9) remains unaltered, and equations (7) and (8) hold provided that the additional pressure terms are considered as included in the $\mathcal{V}$ term. The deviations of $\beta^{\rm est}$ and $M^{\rm est}$ produced by these kinds of pressure may be confined to the central galactic regions, where magnetic fields and active galactic nucleus-related phenomena are more likely to be concentrated.

Additional explanations can be deduced for the deviations of X-ray-derived $\beta^{\rm est}$ and $M^{\rm est}$ from the true values. These include deviations from spherical symmetry, projection/deprojection effects not adequately taken into account, the presence of a multiphase ISM at each radius, and amplification of uncertainties in the process of extracting $T(r)$, $\rho(r)$, $\rho_*(r)$ and $\sigma_{\rm r}(r)$ from the data. However, the possibility is yet to be investigated for these explanations to account at the same time for deviations in β and M, and by precisely the observed amount, as demonstrated here for the hypothesis of lack of hydrostatic equilibrium in the case of NGC 4472.

Our analysis casts doubts on the possibility of using X-ray information and the hydrostatic equilibrium assumption as robust tools to determine accurately the dynamical properties of X-ray-emitting galaxies, at least within $R_{\rm e}$. Another warning to treat X-ray mass estimates with care had already been issued when it appeared that mass models constrained by accurate and extended stellar dynamical data, and including different amounts of dark matter, all lead to similar temperature and X-ray brightness profiles (Bertin et al. 1993), within the uncertainties in the X-ray measurements. In this sense, the situation might be improving with the new *Chandra* and *XMM–Newton* data.

In conclusion, instead of obtaining robust dynamical estimates from hot gas-based studies, it should perhaps be expected that stellar dynamical studies (possibly coupled with gravitational lensing studies) help us to understand the dynamical status of the hot gas.

[3] These selected models also have a velocity dispersion profile consistent with the data for the globular cluster system out to $\sim 2.5 R_{\rm e}$.

ACKNOWLEDGMENTS

We thank G. Bertin for useful discussions and the referee, M. Loewenstein, for comments that improved the paper.

REFERENCES

Bender R., Saglia R. P., Gerhard O., 1994, MNRAS, 269, 785
Bertin G., Toniazzo T., 1995, ApJ, 451, 111
Bertin G., Trenti M., 2003, ApJ, 584, 729
Bertin G., Pignatelli E., Saglia R. P., 1993, A&A, 271, 381
Bertin G. et al., 1994, A&A, 292, 381
Bertin G., Ciotti L., Del Principe M., 2002, A&A, 386, 149
Binney J., Tremaine S., 1987, Galactic Dynamics. Princeton Univ. Press, Princeton, NJ
Camm G. L., 1952, MNRAS, 112, 155
Ciotti L., 1991, A&A, 249, 99
Ciotti L., Lanzoni B., 1997, A&A, 321, 724
Ciotti L., D'Ercole A., Pellegrini S., Renzini A., 1991, ApJ, 376, 380
de Vaucouleurs G., 1948, Ann. Astrophys., 11, 247
Fabbiano G., 1989, ARA&A, 27, 87
Fabricant D., Lecar M., Gorenstein P., 1980, ApJ, 241, 552
Fabricant D., Kent S., Kurtz M. J., 1989, ApJ, 336, 77
Forman W., Jones C., Tucker W., 1985, ApJ, 293, 102
Fridman A. M., Polyachenko V. L., 1984, Physics of Gravitating Systems. Springer-Verlag, Berlin
Fried J. W., Illingworth G. D., 1994, AJ, 107, 992
Gerhard O., Jeske G., Saglia R. P., Bender R., 1998, MNRAS, 295, 197
Hernquist L., 1990, ApJ, 536, 359
Irwin J. A., Sarazin C. L., 1996, ApJ, 471, 683
Jaffe W., 1983, MNRAS, 202, 995

Jones C., Forman W., Vikhlinin A., Markevitch M., David L., Warmflash A., Murray S., Nulsen P. E. J., 2002, ApJ, 567, L115
Kronawitter A., Saglia R. P., Gerhard O., Bender R., 2000, A&AS, 144, 53
Loewenstein M., 1992, ApJ, 384, 474
Mathews W. G., Brighenti F., 2003a, ApJ, 599, 992 (MB03)
Mathews W. G., Brighenti F., 2003b, ARA&A, 41, 191
Merritt D., 1985, AJ, 90, 102
Nipoti C., Londrillo P., Ciotti L., 2002, MNRAS, 302, 901
Osipkov L. P., 1979, SvA, 5, L42
Pellegrini S., Ciotti L., 1998, A&A, 333, 433
Polyachenko V. L., Shukhman I. G., 1981, SvA, 25, 533
Saglia R. P., Bertin G., Stiavelli M., 1992, ApJ, 384, 433
Saha P., 1991, MNRAS, 248, 494
Stiavelli M., Sparke L. S., 1991, ApJ, 382, 466
Sun M., Forman W., Vikhlinin A., Hornstrup A., Jones C., Murray S. S., 2003, ApJ, 598, 250
Thomas P. A., 1986, MNRAS, 220, 949
Tikhonov A. N., Goncharsky A. V., 1987, Ill-posed Problems in the Natural Sciences. MIR, Moscow
Tonry J. L., 1983, ApJ, 266, 58
Trinchieri G., Fabbiano G., Canizares C. R., 1986, ApJ, 310, 637
van der Marel R. P., 1991, MNRAS, 253, 710

This paper has been typeset from a TEX/LATEX file prepared by the author.